Fast Proton Generation from Ultrashort Laser Pulse Interaction with Double-Layer Foil Targets

J. Badziak,[1,*] E. Woryna,[1] P. Parys,[1] K. Yu. Platonov,[2] S. Jabłoński,[1] L. Ryć,[1] A. B. Vankov,[3] and J. Wołowski[1]
[1]*Institute of Plasma Physics and Laser Microfusion, P.O. Box 49, 00-908 Warsaw, Poland*
[2]*St. Petersburg State Technical University, 195251 St. Petersburg, Russia*
[3]*Research Institute for Laser Physics, 199034 St. Petersburg, Russia*
(Received 19 June 2001; published 1 November 2001)

The results of studies of fast-proton generation from foil targets irradiated by 1-ps laser pulse at 10^{17} W/cm^2 are presented. It is shown that a considerable increase in proton energy and current is possible when a double-layer foil target containing a high-Z layer and a low-Z hydrogen-rich layer is used instead of a single-layer target. Proton energies and current increase with the Z of the high-Z layer and depend essentially on the target and the layer thicknesses. Above 10^9 forward-emitted protons of energy >100 keV have been recorded within a cone angle <3°.

DOI: 10.1103/PhysRevLett.87.215001 PACS numbers: 52.38.Kd, 52.50.Jm

Fast protons produced during the interaction of intense ultrashort (≤1 ps) laser pulse with a solid target are a subject of rapidly growing interest due to the possibility of unique applications, particularly in medicine [1,2], material science [3], accelerator technology [4], and nuclear physics on a tabletop [5]. Generation of proton beams by ultrashort-pulse lasers has been experimentally studied by several groups [6–13] with picosecond and subpicosecond laser pulses of intensities from $\sim 10^{17}$ W/cm^2 [6,10] up to 3×10^{20} W/cm^2 [11,12]. Proton energies from ~100 keV to 58 MeV [11] and amounts of protons as high as 3×10^{13} [12] were recorded. These proton beam parameters are much higher than the ones obtained in earlier experiments with high-energy long-pulse lasers [14,15], where protons of maximum energy near 1 MeV were measured.

In the proton experiments with ultrashort-pulse lasers single-layer metal or plastic foil targets were usually used. A proton emission both in the front of [6,9] and behind [8,10–13] a target (in the forward direction) was recorded. No significant influence of the target atomic number (Z) on proton energies was observed; however, several times a greater proton number from the CH target relative to the Au target was measured [11]. In the case of metal targets it was commonly assumed that protons originate from impurity layers on the target surfaces and that they are accelerated by an electrostatic field generated by hot electrons. The experimental results were analyzed and interpreted with the use of particle-in-cell simulations [16,17] and, particularly, the feasibility of focusing the proton beam emitted forward from the back target surface was shown [16]. The above important experimental and theoretical results gave an impulse to formulate a novel scheme of fast ignition for inertial confinement fusion [18] where short-pulse laser-accelerated proton beam focused onto the fusion pellet ignites a compressed nuclear fuel [19].

A key issue for using laser-accelerated protons for fast ignition as well as for their other applications mentioned earlier is reaching high efficiency of proton beam generation, i.e., maximizing proton energies and/or current at a given energy (intensity) of a laser pulse. In this paper we show for the first time that using double-layer thin foil targets containing high-Z front layer and low-Z hydrogen-rich back layer, instead of commonly used single-layer targets, a considerable increase in energies and current of forward emitted protons is possible. The results of the measurements are interpreted in terms of the electrostatic acceleration mechanism assuming that most of the forward accelerated protons originate from the back target surface.

The experiment used a terawatt chirped-pulse-amplification Nd:glass laser [20], generating a 1-ps pulse of short-time scale (<1 ns) intensity contrast ratio $\sim 10^4$ at $\lambda = 1.05$ μm. The linearly polarized laser beam was focused onto thin foil targets, perpendicular to the target surface, with the use of an aspheric lens of the focal length $f = 7.5$ cm. At the best focusing 30%–40% of the laser energy was concentrated in a 10-μm focal spot. Short-lasting ($\sim 10^{-10}$ s) background of the main pulse produced a preplasma of a density scale length comparable to λ [21].

The measurements of ion beam parameters were based on the time-of-flight method and were performed with the use of ion collectors (ICs) and an electrostatic ion-energy analyzer (IEA) [21,22] placed behind the target. The IEA and the ring ion collector IC1 (with a hole in the center) were situated along the laser beam axis and could record ions propagating forward along the target normal. The paths of flights of ions from the target to the IEA and IC1 were 190 and 110 cm, respectively. For rough estimation of the angular distribution of ion emission two additional collectors (IC2 and IC3), viewing the target at angles θ of 26° and 34° with respect to the target normal, were placed 35 cm behind the target. The ion emission measurements were supplemented with the measurement of hard x rays in the range 4–30 keV performed with the use of p-i-n Si photodiode (with 7-μm Al and 1200-μm Be filters), placed behind the target at the angle about 30° with respect to the normal. The measurements were carried out with laser energy up to 0.5 J corresponding to laser intensity on the target 1.5×10^{17} W/cm^2.

In the experiment single-layer and double-layer targets of various Z number and thickness of the layers were applied. Especially, $(C_8H_8)_n$ (polystyrene-PS) and Al foils as well as double-layer targets containing PS foil covered by Au or Cu layers were used. Further, we will use the symbols identifying particular targets which will comprise the letter symbol of the layer (e.g., PS) and the number marking the thickness of the layer in μm (for example, the symbol Au0.05/PS2 will mark the double-layer target containing 2-μm polystyrene layer covered by 0.05-μm Au layer facing towards the laser beam).

Figure 1 presents a typical ion collector signal measured behind Au0.05/PS2 foil in the direction normal to the target surface. As it results from the IC1 and the IEA measurement analysis the ion signal usually consists of three ion groups. The slowest one contains mainly C^+, C^{2+}, and Au^+ ions. The small second group is dominated by C ions with a maximum registered charge state $z = 4+$. The third group practically comprises only fast protons propagating with the peak velocity $\sim(3-4) \times 10^8$ cm/s and the maximum velocity $\sim(7-9) \times 10^8$ cm/s.

To explain details of fast proton generation in our experiment we assume that a general picture of this phenomenon is briefly as follows [12,16]. A high-intensity ultrashort laser pulse interacting with the front of the target produces a short burst of hot electrons. The electrons penetrate through the thin target ionizing H and other atoms at the back target surface where they form a Debye sheath. The negative charge in this sheath is balanced and retained by a positive ion charge sheet. Between the sheath and the ion sheet there is a region of near constant electric field E_{ac} with magnitude $E_{ac} \approx T_h/e\{\max(L_i, \lambda_{Dh})\}$ [11,23], where T_h is the hot electron temperature (in eV), L_i is the ion density scale length, and λ_{Dh} is the hot electron Debye length. Ions in this region and ions from the charge sheet are accelerated by the field. As, typically, $\lambda_{Dh} \sim \mu$m and $T_h \sim 10^4-10^6$ eV, at the sharp density gradient ($L_i < \lambda_{Dh}$) the accelerating field attains high values $\sim 10^4-10^6$ V/μm. The ion acceleration is continued until the hot electrons are energetically depleted, predominantly by accelerating ions; the time (t_{ac}) and the space (L_{ac}) scales for this process are $t_{ac} \sim$ ps and $L_{ac} \sim 10$ μm, respectively. As a result, protons from the back surface are accelerated to energies $E_i \sim 10^5-10^7$ eV.

To be convinced that hot electrons really play a dominant role in the proton acceleration we tried to correlate proton beam parameters with the yield of hard x rays generated predominantly by the hot electrons [24,25]. We found that the x-ray signal growth leads to the increase of both the maximum (E_{max}) and the peak (E_p) proton energies as well as the peak proton current density (j_p), and the increase is especially strong for the proton current density (for definition of E_{max} and E_p see Fig. 1b). Thus, to improve proton beam parameters some conditions for improving the parameters of hot electrons should be created. It can be done particularly by optimization of the atomic number and the structure of a target.

The parameters of a proton beam as a function of a hard x-ray signal for six thin foil targets of various structure and Z number are presented in Fig. 2. First, let us notice that the hard x-ray yields for the double-layer targets with heavy (Au) layer are considerably higher than the ones for the single-layer targets made of lighter elements (PS, Al), and, for instance, for the Au0.05/PS2 target the x-ray yield is above 100 times higher than for the PS2 target. To estimate the effect of the Z number on the hard x-ray yield (X_H) we will compare Au0.05/PS2 and Cu0.05/PS2 targets because of their identical structure. For these targets $X_H^{Au}/X_H^{Cu} \approx 8.1$ and, as a result, $X_H \propto Z^{2.1}$ assuming $X_H(Z)$ dependence as a power function. Such a strong

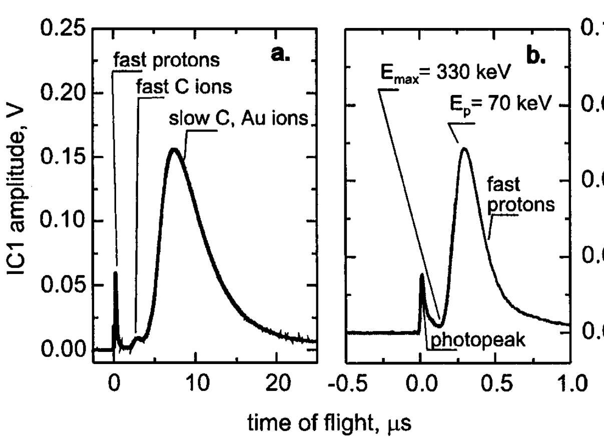

FIG. 1. IC1 collector signal from the Au0.05/PS2 target (a) and the magnified portion of the signal showing the fast proton peak (b). $E_L \approx 0.38$ J, $I_L \approx 10^{17}$ W/cm^2.

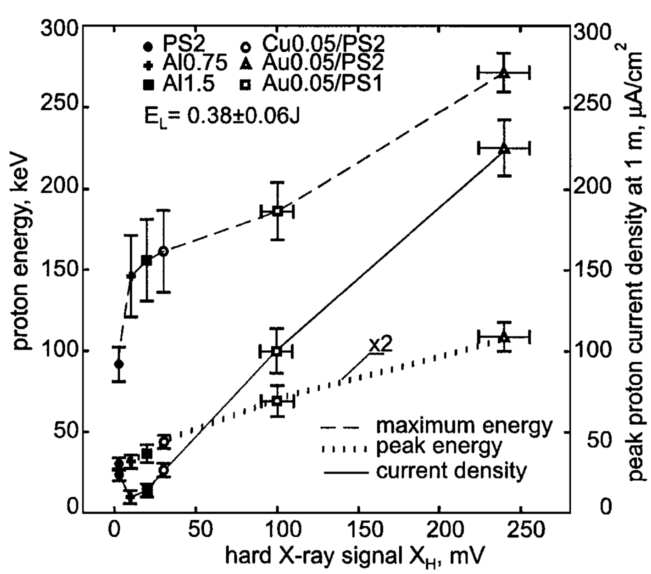

FIG. 2. Parameters of proton beams generated from various single-layer and double-layer targets as a function of hard x-ray signal at fixed energy and intensity of a laser pulse.

dependence $X_H(Z)$ cannot be explained only by an increase of the efficiency of bremsstrahlung emission originating from the fact that the hot electrons traverse a medium of higher Z (this efficiency is roughly proportional to Z [24,25]). Thus, the increase of X_H with the Z number of the layer is likely to originate in part from an increase of number and/or temperature of the hot electrons. It was particularly proved by measurements performed in the papers [26–28] where an increase of the hot electron temperature [26–28] and the hot electron number [28] with Z-number growth was found. So, one can believe that a growth of the temperature together with a probable growth of an amount of hot electrons with the Z number is the main reason for the highest proton energies and currents produced with the Au/PS targets. However, the amount of protons generated depends not only on the Z number of a target but also on the amount of hydrogen in the back side of a target. It is evident from comparison of the results for the hydrogen-rich PS target and Al targets containing only hydrogen adsorbed from contaminants (Fig. 2). In spite of lower Z for the PS proton current density for this target is several times higher than for the Al targets. This result is qualitatively consistent with the one obtained by Snavely *et al.* [11] where 5 times greater proton number from CH target relative to Au target was observed. It should be underlined that some differences in transparency of the PS2 and the Al targets for hot electrons cannot be a reason for lower proton current from Al, because at least the A10.75 target is more transparent than the PS2 target for expected electron energies. Another reason for lower proton current from metal targets can be the existence of free electrons in the metal which can additionally neutralize H ions produced by hot electrons near the back surface.

Parameters of a proton beam recorded behind a target depend on the total target thickness as well as on the thickness of a metal layer covering low-Z foil. The dependencies of E_{max}, E_p, and j_p on the thickness of the PS target are shown in Fig. 3. These dependencies can be understood provided that we realize that before the bulk of the hot electrons is produced by the laser, the target has been heated by an electron heat wave generated by the prepulse and the leading edge of the laser pulse. From a rough estimate using classical heat transport formulas [29,30], for the case of PS target and our pulse parameters we obtain the value $L_T \sim 1\ \mu$m for the characteristic path length (L_T) of the heat wave in the target. Thus, for the thinnest PS target (of thickness $L_{PS} = 0.5\ \mu$m) its back surface is strongly overheated by the heat wave and the ion density scale length L_i is relatively large. The result is a rather low maximum proton energy. On the other hand, the proton current density is high because a great amount of hydrogen at the back side of the target is ionized by the heat wave. In the second extreme case where $L_{PS} = 3.5\ \mu\text{m} > L_T$, the back surface is not overheated and L_i is small. In such a case the electric field

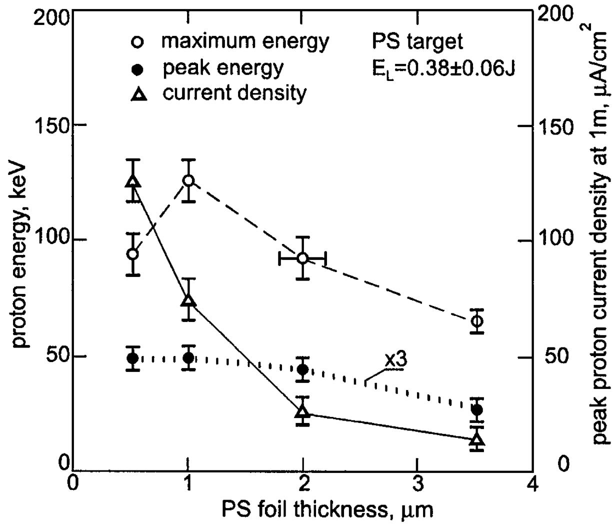

FIG. 3. Parameters of proton beams generated from PS targets as a function of the target thickness.

on the back surface is determined by the Debye length which is estimated to be $\lambda_{Dh} \sim 0.3–0.5\ \mu$m. Thus, for the thicker PS target which would be fully transparent for the hot electrons the energies of protons must be higher than for the thinnest one. However, at $T_h \sim 10$ keV (a rough estimate for PS target) the range of electrons (L_e) in PS is $L_e \sim 2\ \mu$m. If so, the hot electrons are damped in the target of $L_{PS} = 3.5\ \mu$m and both the temperature and the number of the hot electrons on the back surface are lower than in the case of the thinnest target. This, in turn, leads to a decrease of the proton energies. Moreover, at $L_{PS} > L_T$ hydrogen placed near the back surface is ionized only by the hot electrons (not by the heat wave) which, in addition to the lower temperature and the lower number of the hot electrons, results in a considerably lower value of the proton current. The final result is the occurrence of an optimum target thickness (L_{op}), fulfilling the relation $L_T < L_{op} < L_e$ for which the proton energies are near maximum and the lowering of the proton current is not very significant.

The effect of the high-Z layer thickness on the parameters of a proton beam is demonstrated in Fig. 4. When the high-Z layer is very thin, it is evaporated by the laser prepulse before arrival of the main laser pulse. As a result, most of the energy of the pulse is deposited in the low-Z layer and parameters of plasma and the hot electrons are determined mainly by the features of the low-Z medium. Thus, the parameters of a proton beam are close to the ones obtained for a single-layer low-Z target. When, in turn, the high-Z layer is too thick the hot electrons are damped in part in this layer. This reduces the proton energies and the proton current. Therefore, the high-Z layer should be sufficiently thick to absorb the whole laser energy deposited in a target, on the one hand, and it should be thin enough to minimize losses of the hot electrons, on the other hand.

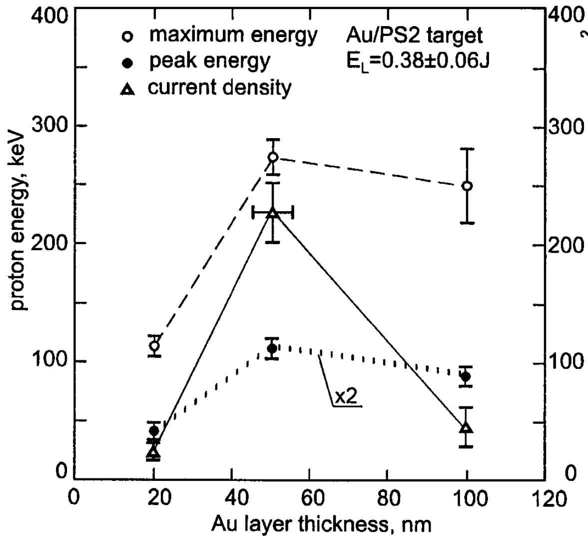

FIG. 4. Parameters of proton beams generated from Au/PS2 targets as a function of Au layer thickness.

Comparing proton signals from the IC1, IC2, and IC3 collectors which record ions emitted at various angles to the target normal, we found that the angular divergence of fast proton emission from Au/PS targets was small and most of the high-energy protons are expected to be emitted in a cone angle smaller than $\sim 30°$ (at angles $\theta \geq 26°$ only protons of energy <10 keV were recorded). High directionality of the proton beam seems to be one of the important reasons for a high proton current density at long distance from the target (L) reaching at $L = 1$ m about 0.4 mA/cm^2 in the case of Au0.05/PS2 target. From the IC1 current measurement we estimated that $>10^9$ protons of energy >100 keV were emitted in a cone angle smaller than 3°.

One of the advantages of double-layer targets, in relation to the single-layer ones, is their flexibility resulting from the fact that the layer "responsible" for hot electron production (the high-Z front layer) and the layer where light ions are produced (the low-Z back layer) can be independently selected and optimized. Particularly, for enhancement of hot electron parameters not only the thickness and Z number but also the structure of the front layer can be optimized. For example, a porouslike structure of the high-Z layer can be used for this purpose [31,32]. The possibility of selection of the back layer parameters and, particularly, the back layer material, creates a prospect for generation light ion beams other than proton beams and, for instance, efficient production of deuteron beams can be expected in the case of Au/CD targets.

In conclusion, we have shown that using double-layer foil targets containing high-Z front layer and low-Z hydrogen-rich back layer, instead of commonly used single-layer targets, a considerable increase in energies and current of protons produced by an ultrashort-pulse laser is possible. Both the maximum and the mean proton energies as well as the proton current are correlated with the hard x-ray yield and they increase with the growth of the Z number of the front layer. Above 10^9 forward-emitted protons of energy >100 keV have been recorded within a cone angle smaller than 3° near the target normal at intensities 10^{17} W/cm^2. For maximizing the proton energies and/or proton current both total target thickness and high-Z layer thickness must be optimally selected. Effectiveness and flexibility of double-layer targets coupled with a possibility of spatial particle beam shaping (e.g., focusing) by curving the back layer surface open up a prospect for construction of efficient tabletop laser-driven accelerators producing high-current-density beams of both protons and other light ions.

This work was supported by the State Committee for Scientific Research (KBN), Poland, under Grant No. 2 P03B 082 019.

*Email address: badziak@ifpilm.waw.pl

[1] J. Raloff, Science News **156**, 257 (1999).
[2] M. I. K. Santala *et al.,* Appl. Phys. Lett. **78**, 19 (2001).
[3] D. S. Gemmel, Rev. Mod. Phys. **46**, 129 (1974).
[4] J. M. de Conto, J. Phys. IV (France) **9**, 115 (1999).
[5] V. Yu. Bychenkov *et al.,* Sov. Phys. JETP **88**, 1137 (1999).
[6] A. P. Fews *et al.,* Phys. Rev. Lett. **73**, 1801 (1994).
[7] F. N. Beg *et al.,* Phys. Plasmas **4**, 447 (1997).
[8] E. L. Clark *et al.,* Phys. Rev. Lett. **84**, 670 (2000).
[9] E. L. Clark *et al.,* Phys. Rev. Lett. **85**, 1654 (2000).
[10] A. Maksimchuk *et al.,* Phys. Rev. Lett. **84**, 4108 (2000).
[11] R. A. Snavely *et al.,* Phys. Rev. Lett. **85**, 2945 (2000).
[12] S. P. Hatchett *et al.,* Phys. Plasmas **7**, 2076 (2000).
[13] A. J. Mackinnon *et al.,* Phys. Rev. Lett. **86**, 1769 (2001).
[14] D. M. Villeneuve *et al.,* Phys. Rev. A **27**, 2656 (1983).
[15] S. J. Gitomer *et al.,* Phys. Fluids **29**, 2679 (1986).
[16] S. C. Wilks *et al.,* Phys. Plasmas **8**, 542 (2001).
[17] A. Pukhov, Phys. Rev. Lett. **86**, 3562 (2001).
[18] M. Tabak *et al.,* Phys. Plasmas **1**, 1626 (1994).
[19] M. Roth *et al.,* Phys. Rev. Lett. **86**, 436 (2001).
[20] J. Badziak *et al.,* Opt. Commun. **134**, 495 (1997).
[21] J. Badziak *et al.,* J. Phys. D **34**, 1885 (2001).
[22] E. Woryna *et al.,* Laser Part. Beams **14**, 293 (1996).
[23] J. Denavit, Phys. Fluids **22**, 1384 (1978).
[24] W. C. Mead *et al.,* Phys. Fluids **26**, 2316 (1983).
[25] J. D. Kmetec, IEEE J. Quantum Electron. **28**, 2382 (1992).
[26] K. B. Wharton *et al.,* Phys. Rev. Lett. **81**, 822 (1998).
[27] J. Yu *et al.,* Phys. Plasmas **6**, 1318 (1999).
[28] L. M. Chen *et al.,* Phys. Rev. E **63**, 036403 (2001).
[29] A. Caruso and R. Gratton, J. Plasma Phys. **11**, 839 (1969).
[30] M. D. Rosen, Proc. SPIE Int. Soc. Opt. Eng. **1229**, 160 (1991).
[31] M. M. Murnane *et al.,* Appl. Phys. B **58**, 261 (1994).
[32] G. Kulcsar *et al.,* Phys. Rev. Lett. **84**, 5149 (2000).